Asian Journal of Chemistry; Vol. 27, No. 4 (2015), 1293-1298

ASIAN JOURNAL OF CHEMISTRY

http://dx.doi.org/10.14233/ajchem.2015.17635

# Hydrogenation of Acetic Acid Over $PtSn/Al_2O_3$ Catalyst: Effect of Shaping Method, Kinetics and Stability

KE ZHANG, HAITAO ZHANG*, HONGFANG MA, WEIYONG YING and DINGYE FANG

Engineering Research Center of Large Scale Reactor Engineering and Technology of the Ministry of Education, State Key Laboratory of Chemical Engineering, East China University of Science and Technology, Shanghai 200237, P.R. China

*Corresponding author: Tel/Fax: +86 21 64252151; E-mail: zht@ecust.edu.cn; zhangke0124@163.com

*Received*: 20 March 2014; *Accepted*: 27 May 2014; *Published online*: 4 February 2015; AJC-16778

The hydrogenation of acetic acid to ethanol is a promising technology for the mass production of ethanol. Two series of $PtSn/Al_2O_3$ catalysts with commercial size were prepared and shaped by different method and tested in the hydrogenation of acetic acid at 275 °C, 2 MPa, LHSV (liquid hourly space velocity) = 0.6 $h^{-1}$ and $n(H_2)/n(CH_3COOH)$ = 12.5. The effect of operation conditions on the performance of one of the catalysts, which shows the highest selectivity of ethanol, was also investigated. After checking the catalyst internal and external diffusion resistance, kinetics of the powdered catalyst was carried out at the following conditions: catalyst 1 g (100-120 mesh), temperature 235-275 °C, pressures 0.5-4.5 MPa, LHSV 0.73-2.18 $h^{-1}$ and $n(H_2)/n(CH_3COOH)$ 2.5-12.5. After that, a 30-days stability test was performed. Kinetics equations derived from a Langmuir-Hinshelwood-type mechanism were established and turn out to be reliable for the hydrogenation of acetic acid over $PtSn/Al_2O_3$ catalyst.

**Keywords: Acetic acid hydrogenation, $PtSn/Al_2O_3$ catalyst, Kinetics, Stability.**

## INTRODUCTION

Nowadays, there is a growing demand for alternatives to petroleum-derived fuels and chemicals due to the consideration of improving air quality and increasing energy security[1,2]. In this context, the research of novel technologies for the production of synthetic fuels and chemicals is gaining attention. Ethanol is being considered as a promising alternative synthetic fuel because it can be produced from biomass and can be used to fuel automobiles or as a potential source of hydrogen for fuel cells[3]. Apart from this, ethanol is also applied in many other fields, such as in the synthesis of a variety of industrial chemicals and polymers, as solvent and antiseptic.

Traditionally, ethanol is mainly produced by two routes: (i) fermentation of biomass, especially sugars that containing six carbons and (ii) hydration of ethylene, which based on petroleum industry[3,4]. The ethylene hydration process, which is carried out by reacting ethylene with steam at 300 °C, 6-7 MPa over a solid catalyst,can get industrial-grade pure ethanol[5]. The fermentation process is not suitable for woody biomass and sugars derived from lignocelluloses and the crude product only contains about 14 % ethanol[6]. From the point of industrial view, both processes are uncompetitive for large-scale ethanol production. The challenge for the former route confronted is the rising of crude oil price and the dependence on imported oil while the disadvantage of latter route is its low energy-efficiency caused by the energy-intensive distillation steps involved in the production of high purity ethanol.

The catalytic conversion of syngas ($CO + H_2$), which derived from the gasification of biomass or coal, could produce ethanol in large quantities. Both homogeneous and heterogeneous catalytic processes have been reported[3]. The homogeneous catalytic processes are in need of expensive catalyst, high operating pressure and tedious workup procedures for catalyst separation and recycling while the heterogeneous catalytic processes exhibit low yield and poor selectivity. Thus, this process remains challenging and no commercial process has been reported though the research on this topic has been proceeding for about a century. However, the production of methanol and its further homogeneous carbonylation to acetic acid are mature technologies[7]. For this reason, the catalytic hydrogenation of acetic acid to ethanol is a promising route, especially suitable for countries with limited farm land and abundant in coal resources, like China.

The study of acetic acid hydrogenation has been conducted by several authors[8-12]. Our former research showed that PtSn catalysts supported on alumina is a good candidate for the production of ethanol from acetic acid hydrogenation and we have studied the role of Sn addition and the effect of Pt/Sn ratio on the performance of the catalysts[13]. The kinetics of

acetic acid hydrogenation is indispensable for the sizing of reactor and the research on this topic is few. Rachmady and Vannice[9-11] have conducted experiments to explore the reaction mechanism of acetic acid hydrogenation, both on $TiO_2$ supported Pt and PtFe catalysts and similar kinetics were obtained based on a Langmuir-Hinshelwood-type model, which involve the dissociation of hydrogen on Pt sites along with the adsorption and activation of acetic acid on oxide phases to create surface acyl species. Catalysts used in commercial process should have appropriate pellet dimension so as to maintain a good physical strength and a suitable pressure drop. In this paper, we compared the performance of two groups of catalysts with commercial size and studied the kinetics of acetic acid hydrogenation over alumina supported PtSn catalyst, as well as its stability.

## EXPERIMENTAL

**Catalysts preparation and characterization:** Two groups of catalysts with commercial size and a given loading (1 wt. % Pt and 1 wt. % Sn) were prepared by co-impregnation. Alumina spheres with a diameter of 3-5 mm were used as support and $H_2PtCl_6.6H_2O$ and $SnCl_4.5H_2O$ were used as precursors for the PtSn catalysts. One group of the catalysts was prepared as follows. After being ground and sieved to 100-120 mesh and calcined at 550 °C for 12 h (in order to remove the organic contaminants), the support was impregnated with aqueous solution of $H_2PtCl_6.6H_2O$ and $SnC1_4.5H_2O$, then the slurry was subject to drying and calcination as described[13]. The catalyst powder was shaped by a tablet press with replaceable moulds and tablets of different size can be obtained. The tablet catalysts were labeled as 1Pt1Sn-T3, 1Pt1Sn-T4 and 1Pt1Sn-T5 where 3, 4, 5 refer to the diameter of the catalysts (mm) and the height of the catalysts is 3 mm. The other group of the catalysts was prepared through the direct impregnation of $Al_2O_3$ spheres with $H_2PtCl_6.6H_2O$ and $SnC1_4.5H_2O$ solution when other steps were the same. Accordingly, the catalysts were labeled as 1Pt1Sn-S3, 1Pt1Sn-S4, 1Pt1Sn-S5 where 3, 4, 5 represent the diameter (mm) of the spheres.

X-Ray diffraction (XRD) of the catalysts was recorded on a Rigaku D/Max 2550VB/PC (Rigaku, Tokyo, Japan, $CuK_\alpha$ radiation). The textural properties of the catalysts were measured by $N_2$ physisorption operated at -196 °C using an ASAP 2020 instrument (Micromeritics, Atlanta, GA). Prior to the adsorption-desorption measurements, the samples were degassed at 200 °C in a $N_2$ flow for 16 h to remove the moisture and other adsorbates.

**Activity testing:** The setup used for the evaluation of acetic acid (99.95 %, Sinopharm Chemical Reagent Co., Ltd, China) hydrogenation is a fixed-bed reactor with an inner diameter of 14 mm, combined with a separation unit and an analysis system. Commonly, 2.8 g catalyst was loaded in the isothermal region of the reactor and reduced in pure $H_2$ (100 mL $min^{-1}$) at 350 °C for 2 h, then the catalyst bed was cooled down to the reaction temperature in 0.5 h. After that, acetic acid was pumped and transported by $H_2$ into the system and preheated to maintain gas phase before entering the reactor. After passing through the condenser and the liquid-vapor separator, the liquid was stored in a tank and the effluent was lead to the analysis system. Compositions of the tail gas were determined on-line and the products in the liquid phase were detected off-line by Agilent 7890A GC (Agilent Technologies, Santa Clara) with a thermal conductivity detector (TCD) and a flame ionization detector (FID). The TCD is furnished with a molecular sieve 5A packed column and a Hayesep Q packed column while the FID is coupled with an HP-PLOT/Q capillary column and an HP-INNOWAX capillary column. Particularly, the acetic acid in the liquid was determined by titration. The performance of the catalysts was tested at a selected condition: t = 275 °C, P = 2 MPa, LHSV (liquid hourly space velocity) = 0.6 $h^{-1}$ and Rm ($n(H_2)/n(CH_3COOH)$) = 12.5. The effect of operation conditions, such as temperature, pressure, LHSV and Rm, on the performance of 1Pt1Sn-T3 was also evaluated. Acetic acid conversion and product selectivity were determined after carbon balance (within ±5 %) was achieved. The calculation of acetic acid conversion and product selectivity was the same as previously described[13].

**Kinetics study and stability:** Kinetics measurements were carried out under the following conditions: catalyst 1 g (100-120 mesh), temperature 235-275 °C, pressures 0.5-4.5 MPa, LHSV 0.73-2.18 $h^{-1}$ and Rm 2.5-12.5, based on the four-factor and five-level orthogonal experimental design. Both the internal and external diffusion effects were eliminated on these kinetics experiments. Stability of the catalyst was tested after the kinetics experiments.

## RESULTS AND DISCUSSION

**Catalysts characterization:** The BET surface area ($S_{BET}$), pore volume ($V_p$) and average pore diameter ($D_p$) of the catalysts and $Al_2O_3$ support are listed in Table-1. The tablet catalysts show a relative higher surface area and a smaller pore diameter, which may be caused by the crush of pores with big diameter during the process of catalyst shaping. On the XRD spectrum (Fig. 1), characteristic diffraction peaks centered at 37.5°, 45.7° and 66.9° are clearly observed, which can be ascribed to $\gamma$-$Al_2O_3$ phase (JCPDS 04-0858)[14]. The absence of Pt, Sn and PtSn alloy phases in our samples may be ascribed to the low loading of Pt, Sn or that Pt and Sn are so highly-

TABLE –1
RESULTS OF $N_2$ PHYSISORPTION

| Catalysts | Surface area ($m^2$ $g^{-1}$) | Pore volume ($cm^3$ $g^{-1}$) | Average pore diameter (nm) |
|---|---|---|---|
| 1Pt1Sn-T3 | 185.2 | 0.42 | 7.7 |
| 1Pt1Sn-T4 | 172.9 | 0.41 | 7.4 |
| 1Pt1Sn-T5 | 159.8 | 0.41 | 7.8 |
| 1Pt1Sn-S3 | 174.7 | 0.40 | 10.0 |
| 1Pt1Sn-S4 | 156.9 | 0.39 | 9.6 |
| 1Pt1Sn-S5 | 133.6 | 0.38 | 9.4 |

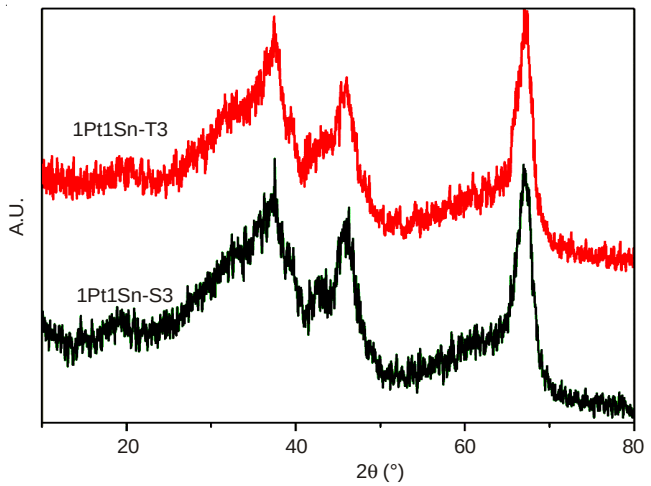


Fig. 1. XRD pattern of the catalysts

dispersed on the alumina support that the size of the crystallite is too small to be detected by XRD characterization[13].

**Performance of the catalysts:** The performance of the commercial-sized catalysts is summarized in Table-2. On one hand, on both catalyst series, the conversion of acetic acid decreased as the diameter increased, which is caused by the decrease of surface area and the selectivity of aldehyde is minor compared to that of ethanol and ethyl acetate, which is because aldehyde is the initial product and can be further hydrogenated. On the other hand, the catalysts directly impregnated with alumina spheres not only show higher acetic acid conversion, but also lead to the production of $CH_4$ and $C_2H_6$, which originate from the decomposition of acetic acid and the hydrogenation of the ethanol[9]. Both phenomena can be explained in terms of the different metal distribution behaviour caused by the preparation procedure. For catalysts impregnated with alumina spheres, the distribution of metals is inhomogeneous, being eggshell-typed, *i.e.* the concentration of metals is gradually decreased from the outer layer to the core of the alumina sphere[15]. However, the distribution of metal precursors is homogeneous on the tablet catalysts. For industrial catalysts, the appearance of by-product should be prevented and suitable operating conditions are indispensable. Consequently, 1Pt1Sn-T3 was selected to investigate the effect of operating conditions on the performance of acetic acid hydrogenation.

**Effect of temperature:** The effect of temperature on acetic acid conversion and product selectivity over catalyst 1Pt1Sn-T3 is shown in Fig. 2, where HOAc represents acetic acid, AH aldehyde, EtOH ethanol and EtOAc ethyl acetate. It is evident that the rise of temperature is beneficial to the conversion of acetic acid and the selectivity of ethyl acetate and detrimental to the product of ethanol. The enhancement of acetic acid conversion is due to the promotion of reaction rate caused by the rise of temperature while the changes of product selectivity can be attributed to the difference of activation energy.

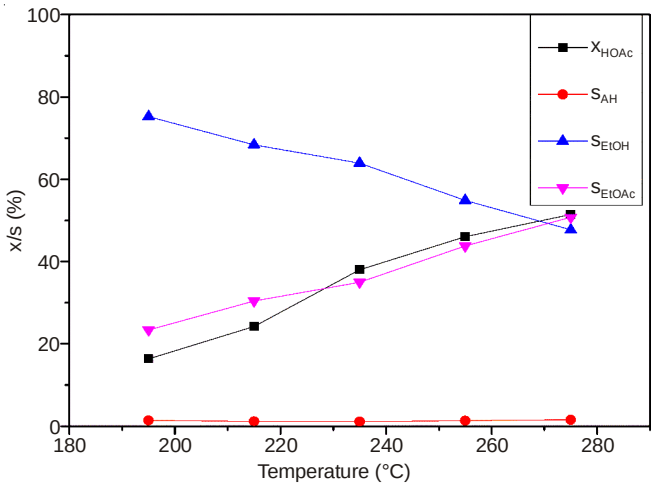


Fig. 2. Effect of temperature on the performance of catalyst 1Pt1Sn-T3

**Effect of pressure:** The influence of pressure on the conversion and product selectivity over catalyst 1Pt1Sn-T3 is present in Fig. 3. The conversion of acetic acid rose along with the increase of pressure, which is result from the enhanced density of active acetate surface species and the improved collision probability of reactants and catalyst. At the same time, the selectivity of ethanol increased while that of ethyl acetate decreased. The reduction of acetic acid to ethanol and the

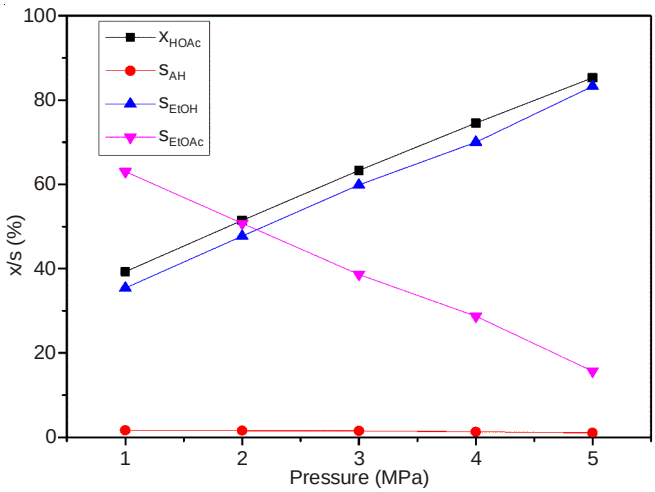


Fig. 3. Effect of pressure on the performance of catalyst 1Pt1Sn-T3tec

TABLE-2
PERFORMANCE OF THE CATALYSTS

| Sample | Conversion (%) | Selectivity (%) | | | | |
|---|---|---|---|---|---|---|
| | | $CH_3CHO$ | $C_2H_5OH$ | $C_2H_5OCOCH_3$ | $CH_4$ | $C_2H_6$ |
| 1Pt1Sn-T3 | 51.4 | 1.9 | 47.7 | 50.4 | - | - |
| 1Pt1Sn-T4 | 39.9 | 1.8 | 42.0 | 56.2 | - | - |
| 1Pt1Sn-T5 | 30.9 | 2.1 | 37.7 | 60.1 | - | - |
| 1Pt1Sn-S3 | 52.2 | 1.6 | 39.9 | 53.2 | 7.5 | 1.6 |
| 1Pt1Sn-S4 | 47.5 | 1.5 | 39.7 | 50.7 | 7.8 | 1.5 |
| 1Pt1Sn-S5 | 44.9 | 1.4 | 38.4 | 51.3 | 7.2 | 1.6 |

esterification of acetic acid and ethanol to ethyl acetate are two consecutive reactions in the system. The former one is a molecules reduced reaction while the latter one is an equimolecular reaction. Thus, the increase of pressure is beneficial to the production of ethanol.

**Effect of liquid hourly space velocity (LHSV):** Fig. 4 displays the effect of LHSV on the conversion of acetic acid and product selectivity. The changes caused by the rise of LHSV are minor: the conversion of acetic acid and selectivity of ethyl acetate saw a slight decline while the selectivity of ethanol was prompted a bit. The higher the LHSV, the shorter the contact time between the reactants and the catalyst surface. Consequently, the above-mentioned behaviour was observed.

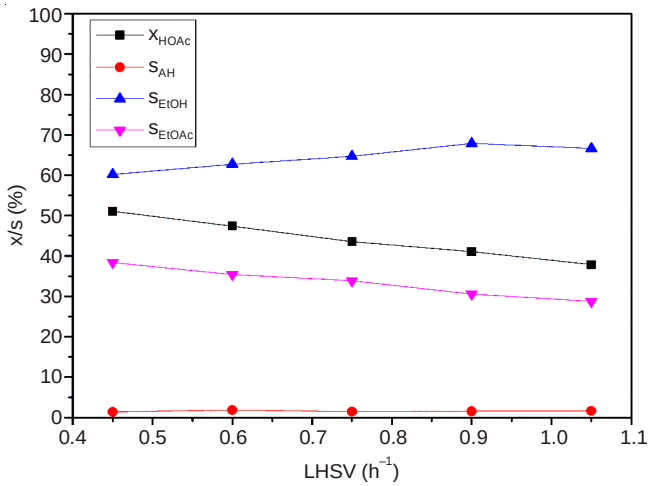


Fig. 4. Effect of LHSV on the performance of catalyst 1Pt1Sn-T3

## Kinetics of hydrogenation of acetic acid

**Kinetics model assumptions:** Rachmady and Vannice[9] had studied the kinetics of hydrogenation of acetic acid over $Pt/TiO_2$ catalysts and a final rate expression was obtained. The experiments were carried out at a low acetic acid conversion and the products they considered were aldehyde, ethanol and ethane. In present case, the acetic acid conversion is in the range of 5-65 % and the selectivity of aldehyde is about 1 % while the selectivity of ethyl acetate is considerable. Thus, the reactions we considered are the hydrogenation of acetic acid to ethanol and the esterification of ethanol with acetic acid to ethyl acetate.

$$CH_3COOH + 2H_2 = C_2H_5OH + H_2O \quad (1)$$

$$CH_3COOH + C_2H_5OH = C_2H_5OCOCH_3 + H_2O \quad (2)$$

The elementary steps involved in reaction 1 are eqn. 3-12 while the elementary steps related to eqn. 2 are eqn. 13 and 14. Briefly, eqn. 3-5 in the reaction sequence represent the dissociative adsorption of hydrogen on Pt surface, followed by the migration of H atoms from the metal to the oxide surface, as well as the dissociative adsorption of acetic acid, where * is an active site on the Pt surface, sp denotes the transfer of H atoms from the metal to the oxide surface. Eqn. 6 depicts the molecular adsorption of acetic acid, where S represents a site on the oxide surface. After a series of irreversible surface reactions, *i. e.* the consecutive addition of adsorbed hydrogen atoms to the adsorbed acetic acid molecule, aldehyde is formed as the initial product, which can either desorb or be hydrogenated to ethanol. Subsequently, the formed ethanol can desorb or react with the adsorbed acetic acid molecule to form ethyl acetate. These surface reactions and reversible desorption steps are depicted by eqns. 7-14 and the rate-determining steps of reaction 1 and 2 are eqn. 7 and 13, respectively.

$$H_{2(g)} + 2* \overset{K_{H_2}}{\rightleftharpoons} 2H* \quad (3)$$

$$H* \overset{K_{sp}}{\rightleftharpoons} H_{sp} \quad (4)$$

$$CH_3COOH_{(g)} + 2* \overset{K_{Ac}}{\rightleftharpoons} CH_3COO* + H* \quad (5)$$

$$CH_3COOH_{(g)} + S \overset{K_{HOAc}}{\rightleftharpoons} CH_3COOH\text{-}S \quad (6)$$

$$CH_3COOH\text{-}S + H_{sp} \xrightarrow{k_1'} CH_3COOH_2\text{-}S \quad (7)$$

$$CH_3COOH_2\text{-}S + H_{sp} \xrightarrow{k_2'} CH_3CHO\text{-}S + H_2O_{(g)} \quad (8)$$

$$CH_3CHO\text{-}S \underset{k_{-3}'}{\overset{k_3'}{\rightleftharpoons}} CH_3CHO_{(g)} + S \quad (9)$$

$$CH_3CHO\text{-}S + H_{sp} \xrightarrow{k_4'} CH_3CHOH\text{-}S \quad (10)$$

$$CH_3CHOH\text{-}S + H_{sp} \xrightarrow{k_5'} CH_3CH_2OH\text{-}S \quad (11)$$

$$CH_3CH_2OH\text{-}S \overset{K_{EtOH}}{\rightleftharpoons} CH_3CH_2OH_{(g)} + S \quad (12)$$

$$CH_3CH_2OH - S + CH_3COOH - S \xrightarrow{k_6'} CH_3CH_2OCOCH_3 - S + H_2O_{(g)} + S \quad (13)$$

$$CH_3CH_2OCOCH_3\text{-}S \underset{k_{-7}'}{\overset{k_7'}{\rightleftharpoons}} CH_3CH_2OCOCH_{3(g)} + S \quad (14)$$

The hydrogenation activity is determined by the rate of acetic acid disappeared to form hydrogenated products, *i.e.* the overall formation rate of acetaldehyde, ethanol and ethyl acetate. Applying the steady-state approximation to the surface intermediates, the final rate expressions can be written as 15-17.

$$r_1 = k_1'\theta_{HOAc}C_H \quad (15)$$

$$r_2 = k_6'\theta_{HOAc}\theta_{EtOH} \quad (16)$$

$$r_{HOAc} = r_1 + r_2 \quad (17)$$

where $\theta_i$ is the fractional surface coverage of species i, the subscript HOAc and EtOH represents the acetic acid and ethanol molecules adsorbed on the oxide respectively and $C_H$ is the concentration of hydrogen atoms at this site on the oxide surface. The total number of active sites are incorporated in $k_1$ and $k_6$.

The dissociative adsorption of hydrogenation and acetic acid on the Pt surface are quasi-equilibrated and can be expressed as:

$$K_{H_2} = \theta_H^2 / P_{H_2}\theta_*^2 \quad (18)$$

$$K_{Ac} = \theta_{Ac}\theta_H / P_{HOAc}\theta_*^2 \quad (19)$$

where subscripts * and Ac represent vacant sites and acetate on the Pt surface, respectively, while $P_i$ and $K_i$ are the partial pressure and adsorption equilibrium constant of species i, respectively. The quasi-equilibrium expressions for acetic acid and ethanol adsorption and H atom concentration at the oxide surface site are written as

$$K_{HOAc} = \theta_{HOAc}/P_{HOAc}\theta_S \quad (20)$$

$$K_{EtOH} = \theta_{EtOH}/P_{EtOH}\theta_S \quad (21)$$

$$K_{sp} = C_H/\theta_H \quad (22)$$

where sp represents the migration of adsorbed H from Pt sites to the surface of oxides. Based on the following assumptions: adsorbed hydrogen atoms (H*) and adsorbed acetate species ($CH_3COO$*) are the predominant surface species on Pt and molecular acetic acid and ethanol are the significant surface intermediates on the oxide surface sites, the expressions can be obtained.

$$\theta_* = 1/(\sqrt{K_{H_2}P_{H_2}} + K_{AC}P_{HOAc}/\sqrt{K_{H_2}P_{H_2}}) \quad (23)$$

$$\theta_s = 1/(1 + K_{HOAc}P_{HOAc} + K_{EtOH}P_{EtOH}) \quad (24)$$

After resolving equation group (13-22), the final rate expressions are obtained

$$r_1 = \frac{k_1 P_{HOAc}\sqrt{P_{H_2}}}{(1+K_3P_{HOAc}+K_4P_{EtOH})(K_1\sqrt{P_{H_2}}+K_2P_{HOAc}/\sqrt{P_{H_2}})} \quad (25)$$

$$r_2 = \frac{k_2 P_{HOAc}P_{EtOH}}{(1+K_3P_{HOAc}+K_4P_{EtOH})^2} \quad (26)$$

where

$$k_1 = k_1'K_{HOAc}K_{sp}\sqrt{K_{H_2}} \quad (27)$$

$$k_2 = k_6'K_{HOAc}K_{EtOH} \quad (28)$$

$$K_1 = \sqrt{K_{H_2}} \quad (29)$$

$$K_2 = K_{AC}/\sqrt{K_{H_2}} \quad (30)$$

$$K_3 = K_{HOAc} \quad (31)$$

$$K_4 = K_{EtOH} \quad (32)$$

$k_1$ and $k_2$ are reaction rate constants and the temperature dependence of the rate constants is expressed by the Arrhenius' law,

$$k_i = k_{0,i}\ \exp(-E_{a,i}/RT)(i = 1,2) \quad (33)$$

while

$$K_i = \exp(a_i + b_i/RT)(i = 1, 2, 3, 4) \quad (34)$$

The reaction rate was tested in the isothermal integral fixed bed reactor. Preliminary tests were carried out to check the catalyst internal and external diffusion resistance. The influence of the internal diffusion was investigated by performing experiments on catalyst of different pellet sizes in identical working conditions. To check for external diffusion resistance, several tests were carried out at different acetic acid flow rates, keeping constant the catalyst weight[16]. The acetic acid conversion showed that, during the working domain, the influence of external diffusion on process kinetics is not obvious. Finally, the kinetic study was performed under the following condition: catalyst 1 g (100-120 mesh), temperature 235-275 °C, pressures 0.5-4.5 MPa, LHSV 0.73-2.18 $h^{-1}$ and Rm 2.5-12.5. Reaction rate can be obtained as follows:

$$\frac{dN_{HOAc}}{dw} = -\frac{d(N_{HOAc,0}(1-x_{HOAc}))}{dw} = N_{HOAc,0}\frac{dx_{HOAc}}{dw} \quad (35)$$

Acetic acid conversion in the reactor outlet can be expressed as follows:

$$x = \int_0^w \frac{r}{N_{HOAc,0}}dw \quad (36)$$

The production rate of ethyl acetate is

$$r_2 = \frac{dN_{EtOAc}}{dw} = \frac{N_{HOAc,0}d(x_{HOAc}(1-s_{EtOH}))}{2dw} = \frac{N_{HOAc,0}}{2}\left(\frac{(1-s_{EtOH})dx_{HOAc} - x_{HOAc}ds_{EtOH}}{dw}\right) \quad (37)$$

where s represents selectivity. After a simple algebraic transformation, eqn. 37 can be write as:

$$\frac{ds_{EtOH}}{dw} = \frac{(1-s_{EtOH})r_1 - (1+s_{EtOH})r_2}{x_{HOAc}N_{HOAc,0}} \quad (38)$$

Acetic acid conversion and the selectivity of ethanol in the reactor outlet can be obtained by integrating eqns. 36 and 38. Discrimination of the kinetic model was performed by fitting the experimental data to the kinetics eqns. 25 and 26. The estimation of the values of the kinetics parameters through best-fit methods was determined with a multivariable nonlinear regression method, using the Levenberg-Marquardt algorithm. The objective function was to minimize the sum of the square of residuals corresponding to the differences between the experimental data and those calculated data for the kinetic model. It was found that the kinetics equations fit well to the experimental data.

**Estimation of the kinetics parameters:** Since the reaction rate was tested in an isothermal integral fixed bed reactor, the process taking place inside the catalyst bed was described by the pseudo-homogeneous fixed bed reactor model[16]. The activation energy of the reactions and other kinetics parameters can be obtained using the Levenberg-Marquardt algorithm and the results are represented in Table-3.

TABLE-3
ESTIMATED KINETICS PARAMETERS

| Parameter | Estimated value |
|---|---|
| $k_{1,0}$ (mol $g^{-1}$ cat $h^{-1}$) | 3.43 |
| $E_{1,a}$ (J $mol^{-1}$) | -78429.5 |
| $k_{2,0}$ (mol $g^{-1}$ cat $h^{-1}$) | 744.52 |
| $E_{2,0}$ (J $mol^{-1}$) | -35805.5 |
| $a_1$ | 50.39 |
| $b_1$ | -57663.3 |
| $a_2$ | -153.82 |
| $b_2$ | 55877.24 |
| $a_3$ | -80.58 |
| $b_3$ | 50471.95 |
| $a_4$ | -154.49 |
| $b_4$ | 111185.1 |

**Verification of the model:** It is stated that the kinetics model is suitable when $F > 10 \times F_{0.05}$, $\rho^2 > 0.9$. Statistic results in Table-4 shows that kinetics eqns. 25 and 26 meet the requirements above. The parity plot of all the data compared to the model estimations with the use of the kinetics eqns 25, 26 are given in Fig. 5. The distribution of the points in this diagram indicates a reasonably good quality of fitness of our experimental data, by the kinetics eqn 25, 26. Therefore, the kinetics eqn. 25 and 26 are suitable for this experiment.

TABLE-4
STATISTIC RESULTS OF THE KINETICS MODEL

| Equation | Mp | M-Mp | $\rho^2$ | F | $F_{0.05} \times 10$ |
|---|---|---|---|---|---|
| (25) | 10 | 15 | 0.997 | 497.81 | 25.4 |
| (26) | 6 | 19 | 0.997 | 992.91 | 25.1 |

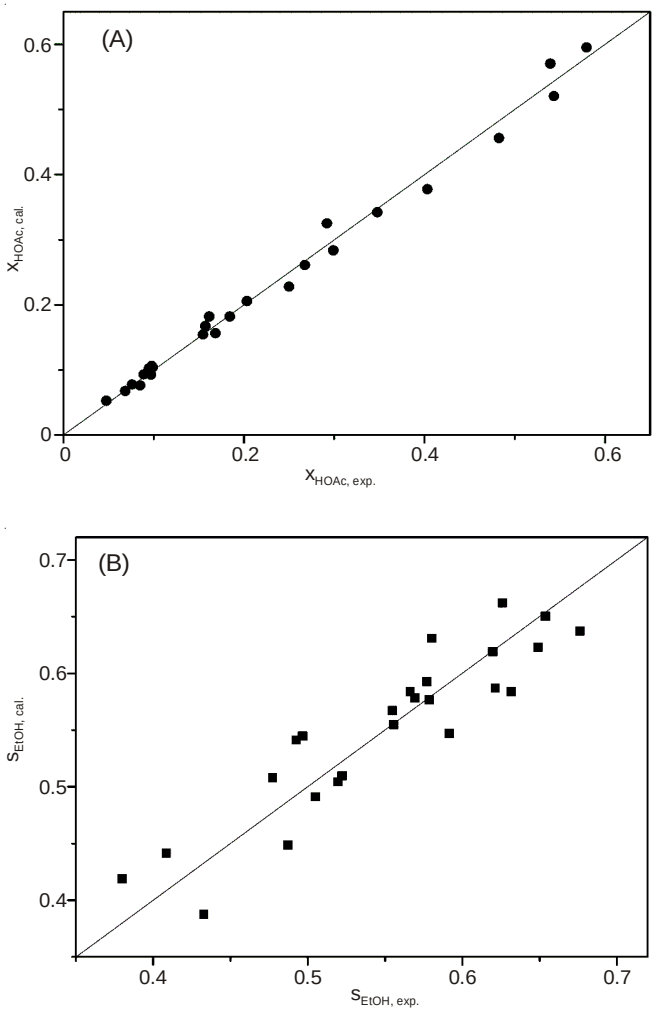


Fig. 5. Calculated values *versus* experimental values: (A) the conversion of acetic acid and (B) the selectivity of ethanol

**Catalyst stability:** From the perspective of industrial view, a suitable catalyst should have a good stability[15]. Therefore, after the kinetics study, the catalyst was subjected to 30-days stability test under the condition: 255 °C, 2.5 MPa, LHSV = 1.8 $h^{-1}$ and Rm = 10 and the result is shown in Fig. 6. It can be seen that the catalyst shows a good stability, the conversion of acetic acid dropped about 4.5 % over 30 days and the selectivity of ethanol and ethyl acetate fluctuates slightly.

## Conclusion

Two groups of commercial-sized $PtSn/Al_2O_3$ catalysts were prepared and their physical properties were characterized. Activity testing shows that catalysts impregnated with alumina spheres are more active and produce about 10 % by-products ($CH_4 + C_2H_6$) under the selected reaction condition. The effect of operation conditions on the performance of the catalyst

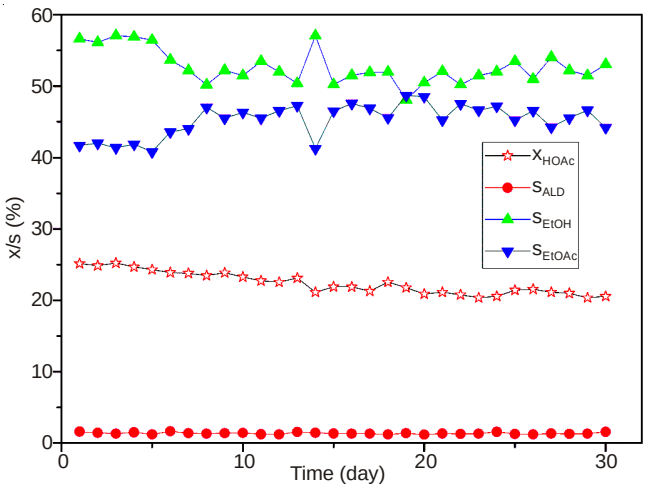


Fig. 6. Stability plot of the catalyst

1Pt1Sn-T3 was analyzed and the results exhibit that temperature and pressure had significant effect on the conversion of acetic acid and the selectivity of ethanol and ethyl acetate while LHSV and molar ratio had minor impact on the performance of the catalyst under the laboratory conditions. The kinetics eqns. 25 and 26 derived from a Langmuir-Hinshelwood-type mechanism are reliable for acetic acid hydrogenation over $PtSn/Al_2O_3$ catalyst. At the same time, the catalyst also displayed a quite good stability. During the 30 days experiment, the acetic acid conversion dropped from 25.1 to 20.6 % while the product selectivity fluctuated slightly.

## ACKNOWLEDGEMENTS

This work is financially supported by the National Science and Technology Supporting Plan (2006BAE02B02).

## REFERENCES

1. G. Berndes, C. Azar, T. Kåberger and D. Abrahamson, *Biomass Bioenergy*, **20**, 371 (2001).
2. A.E. Farrell, R.J. Plevin, B.T. Turner, A.D. Jones, M. O'Hare and D.M. Kammen, *Science*, **311**, 506 (2006).
3. V. Subramani and S.K. Gangwal, *Energy Fuels*, **22**, 814 (2008).
4. B.D. Solomon, J.R. Barnes and K.E. Halvorsen, *Biomass Bioenergy*, **31**, 416 (2007).
5. C.M. Fougret and W.F. Hölderich, *Appl. Catal. A*, **207**, 295 (2001).
6. J.R. Rostrup-Nielsen, *Science*, **308**, 1421 (2005).
7. N. Yoneda, S. Kusano, M. Yasui, P. Pujado and S. Wilcher, *Appl. Catal. A*, **221**, 253 (2001).
8. G. Onyestyák, S. Harnos, S. Klébert, M. Stolcová, A. Kaszonyi and D. Kalló, *Appl. Catal. A*, **464-465**, 313 (2013).
9. W. Rachmady and M.A. Vannice, *J. Catal.*, **192**, 322 (2000).
10. W. Rachmady and M.A. Vannice, *J. Catal.*, **209**, 87 (2002).
11. W. Rachmady and M.A. Vannice, *J. Catal.*, **207**, 317 (2002).
12. R. Pestman, R.M. Koster, J.A.Z. Pieterse and V.J. Ponec, *J. Catal.*, **168**, 255 (1997).
13. K. Zhang, H.T. Zhang, H.F. Ma, W.Y. Ying and D.Y. Fang, *Catal. Lett.*, (2014). (In press).
14. J.L. Ayastuy, M.P. González-Marcos and M.A. Gutiérrez-Ortiz, *Catal. Commun.*, **12**, 895 (2011).
15. Z.T. Huang and J.M. Geng, Industrial Catalysis, Chemical Industry Press, Beijing, p.185 (2006).
16. G.F. Froment and K. Bischoff, Chemical Reactor Analysis and Design, John Wiley & Sons, Inc., New York, p. 428 (2011).